MODELLING THE FLOW OF HYDROTHERMAL FLUIDS ABOVE AN EVOLVING CONTINENTAL RIFT

Warwick Kissling[1], Susan Ellis[2]

[1] Industrial Research Limited, PO Box 31310, Lower Hutt, New Zealand.

[2] GNS Science, 1 Fairway Drive, PO Box 30368, Lower Hutt, New Zealand.

w.kissling@irl.cri.nz, s.ellis@gns.cri.nz

Keywords: *Continental rift, hydrothermal fluids,*

ABSTRACT

We use a thermo-mechanical code (SULEC) to model the evolution and deformation of a continental rift over millions of years. We use SULEC to predict the change in crustal properties and the evolution in the brittle-ductile transition. For a specified SULEC output time, the basal heat-flow, material properties, degree of melting, brittle and ductile material evolution and rift geometry and an inferred permeability distribution for the upper 30 km of the crust are passed to TOUGH2, and the evolution of fluid flow is followed for 200 kyr. This one-way coupling allows us to examine the changing fluid flow regime predicted by TOUGH2 for the crust as the rift evolves.

We find that the spatially evolving brittle-ductile transition predicted by SULEC has a strong influence on the fluid flow regime predicted by TOUGH2. Since the brittle-ductile transition depends on temperature, pressure, ambient strain-rates, and fluid pressure, we can demonstrate the feedback between deformation and crustal fluid flow for an evolving rift such as the Taupo Volcanic Zone (TVZ). In particular, it appears that the formation of hydrothermal plumes is favoured when the crustal permeability is greater than ~10^{-15} m^2 and when the ratio of brittle/ductile (B/D) permeabilities in the crust is ~10. Conversely, for lower crustal permeabilities, and lower B/D permeability ratios, hydrothermal plume formation is suppressed. In addition, the development of partial melt predicted by SULEC changes the flux of heat and fluid into the TOUGH model in time.

1. INTRODUCTION

Most existing models of hydrothermal circulation in magmatic rifts have not considered evolution of the rift, yet rift structure can have a key influence on fluid flow through permeability changes due to strain (e.g. faults), stress and strainrate (porosity, brittle vs. ductile processes), and stratigraphy (e.g., Rowland and Sibson, 2004; Kissling et al., 2009). Features of the hydrothermal system that may be affected by rift structure include the nature and source of recharge, timescales of formation and stability of hydrothermal plumes, the spatial relation of plumes to underlying magma bodies and zones of active faulting, and the transfer mechanisms from magmatic source to hydrothermal systems.

In this paper we give a progress report on linking a geodynamic code SULEC (Ellis et al., in press) to a fluid flow code TOUGH2 (Pruess, 1991) to study the effect of an evolving rift on hydrothermal circulation. We loosely base our model constraints on the evolving Taupo rift.

We show how the evolution in rift structure, particularly the variation in depth of the brittle-ductile transition and the formation of partial melt, can influence the resulting hydrothermal plume formation. For the preliminary steps reported here, we make no attempt to "tune" our models to the natural example of TVZ, but rather demonstrate the effect of the evolving rift on fluid circulation as a "proof of concept".

2. CONSTRAINTS FROM THE TAUPO RIFT

Pertinent constraints from the TVZ include:

- Current extension rate ca. 12 mm/year (Wallace et al., 2004). Rifting began ca. 2 Ma (Wilson et al., 1995).
- Total TVZ heat flux ca. 4000 MW, discharged via ~20 high temperature geothermal fields (Bibby et al., 1995). Average heat flux ~ 700 mW/m^2 (Bibby et al., 1995).
- The geothermal systems appear to be stable for periods of ~ several hundred kyr. (e.g. Grindley, 1965, Browne 1979.)
- 3D inversions of MT data suggest extensive zones of partial melt at mid-crustal depths > 13 km, and ca. 10km across. Most of these run beneath the active (narrow) rift (Figure 1b) (Heise et al., 2010).
- Depth of the brittle-ductile transition (BDT) based on seismogenic zone, is 6-8 km within the Taupo rift (Bryan et al., 1999), and somewhat deeper outside (Hayes et al., 2004; Sherburn and White, 2005).
- Width of rift has narrowed over time (Villamor et al., in prep). The young rift (ca. 300 ka) is focused on the Taupo Fault Belt (< 20 km across). Old rift bounding faults are ca. 40-80 km apart. The narrowing of the rift has been accompanied by a shift in the locus and style of volcanism (Wilson et al., 1995).

3. MODEL DESCRIPTION

3.1 Thermo-mechanical code

We use the thermo-mechanical code SULEC to solve the incompressible Stokes equation for slow creeping flow together with the heat equation. Thermal diffusion and advection are computed at each timestep. Pressure (mean stress) is calculated through an iterative penalty formulation (Pelletier et al., 1989). The Eulerian grid on which the computation is performed does not deform horizontally but stretches vertically to account for topographic changes at the upper free surface. Materials, strain and stress fields are advected via tracer particles.

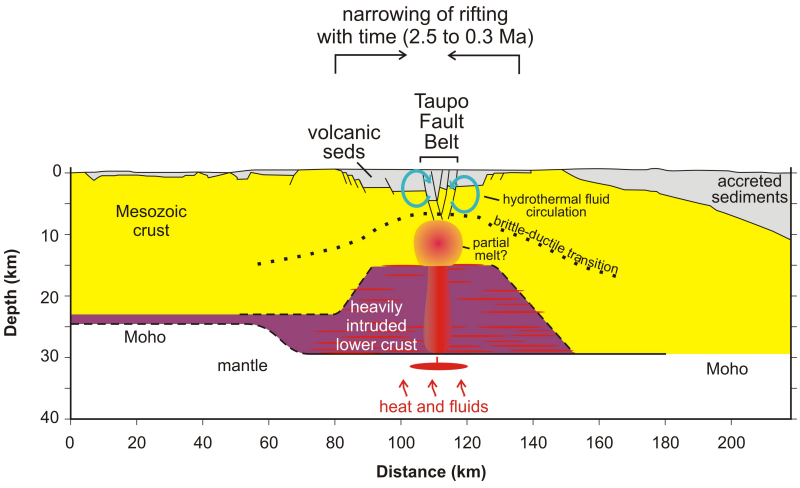


Figure 1. Cartoon summarising some of the main features of the Taupo Volcanic Zone, based loosely on a cross-section through the Taupo region. Dotted line shows conjectured brittle-ductile transition shallowing beneath rift. Modern rifting is concentrated in a narrow zone (the Taupo Fault Belt). The zone of partial melt schematically represents the magnetotelluric conductivity anomaly C1 from Heise et al., (2010). The rest of the figure is simplified from Harrison and White (2006); Rowland and Sibson (2001); Rowland et al., (2010), Eberhart-Phillips et al., (2008); Bibby et al., (2008); Bryan et al., (1999); Villamor et al., (in prep). The vertical exaggeration is 2x.

The modelled domain for the thermo-mechanical calculations is 300 km wide and 120 km deep (Figure 2) with a grid spacing of 2×2 km and ca. 4 tracer particles per element. The 30 km-thick crustal layer has pressure-sensitive frictional Coulomb yield (internal angle of friction and cohesion as detailed in Table 1) giving way to thermally-controlled ductile flow (Table 1; crust ductile parameters based on Gleason and Tullis, 1995). We assume that rocks weaken with strain to represent effects of brittle fault development and softening due to, for example, cohesion loss, mineral phase changes, elevated pore fluid pressures, grain size reduction and/or the development of foliation. The transition from brittle to ductile yield occurs at the point where brittle and ductile strengths are equal, which evolves naturally during the model run at each location depending on ambient effective pressure, temperature and strain-rates. Similar rheological properties are prescribed for the mantle, except that the ductile flow parameter values are derived from laboratory experiments on wet olivine (Freed and Burgmann, 2004).

Viscosities in the crust and mantle are modified where melt is present based on a relative fall-off in viscous strength between temperature limits Tm_1 and Tm_2. We determine a melt fraction f as a function of temperature (and for the mantle, pressure), which then alters density and viscosity of the material as detailed in Table 2 (from arguments given in Gerya and Yuen (2003)). These relationships are a simplification of real melt development and a better method would involve lookup tables that correctly model mineral phase equilibria for each temperature, pressure and fluid content (e.g., Ellis et al., in press). When melt is present at the calculated pressure and temperature, latent heat is included in the thermal calculation via an increased effective heat capacity (Gerya and Yuen, 2003).

Velocity boundary conditions are applied to the sides of the model whereby the top 90 km moves symmetrically outwards to impose rifting of the lithosphere. Beneath this depth we impose an oppositely directed boundary condition to balance inflow with outflow. The base has zero vertical displacement but is free to move horizontally. The top is a free surface with isostatic stabilisation (Kaus et al., 2010; Quinquis et al., 2011). A basal heat-flow of 30 mW m^{-2} increases to 100 mW m^{-2} in a 15-km-wide region at the centre of the model, and an upward fluid flux of 1.6 cm yr^{-1} is also imposed in this region, to simulate a pulse of heat and fluids from underlying subducting sediment (the actual subduction process is not modeled). No surface erosion or sedimentation is applied.

Table 1. Rheological parameter values for SULEC

	Pre-exponential constant (MPa $^{-n}$ s^{-1})	Activation energy (kJ mol^{-1})	Power-law exponent
SULEC crust[1]	1.1×10^{-4}	223	4
SULEC mantle[1]	3.6×10^{5}	480	3.5
	Friction angle (°)	Frictional cohesion (MPa)	Density (kg m^{-3})
SULEC crust[1]	35 to 5[2]	1	2800
SULEC mantle[1]	35 to 5[2]	1	3300

[1]Ductile viscosity parameters for no partial melt; correct geometrical factor to translate from triaxial laboratory experiments to plane-strain is calculated separately.
[2]Softening linearly between these limits as total strain increases from 5% and 100%. Effective pressure (total pressure minus fluid pressure) is used in frictional calculations.

We model an initial quiescent tectonic period of 2 My where the total extensional velocity imposed is 0.2 cm yr^{-1}, representing the stage where a pulse of heat and fluid flux from the subduction zone are gradually impinging on the nascent rift. Following this, the centre of the model has become thermally weakened. We then impose the full rift velocity of 1 cm yr^{-1} and follow the development of localised shear zones (representing rift flanking faults) and evolution in strain-rate and the brittle-ductile transition in time. At selected times during rift evolution, this information is passed to the fluid code, as described below.

Table 2. Effect of partial melt fraction *f* on rheological parameters in SULEC

	Tm_1 (°C)[1]	Tm_2 (°C)	Latent heat of melting (kJ/kg)
SULEC crust	700	800	300
SULEC mantle	1240+49800 /(*P*+323)	2073+0.11 4*P*	400
	Density (kg m^{-3})	Viscosity (Pa s)	
SULEC crust	2800-600*f*	Maximum of: 10^{18}; 10^{16}.exp[2.5+((1-f)/f)$^{0.48}$(1-f)]	
SULEC mantle	3300-400*f*	Maximum of: 10^{18}; 10^{16}.exp[2.5+((1-f)/f)$^{0.48}$(1-f)]	

[1]*P* is total pressure in MPa

Table 3. Thermal parameter values in SULEC

	Thermal conductivity (W m^{-1} K^{-1})	Heat capacity (KJ kg^{-1} K^{-1})	Heat production (μW m^{-3})
SULEC crust	2.84	1.1	1
SULEC mantle	2.84	1.1	0

3.2 Fluid flow code

An extended version of the geothermal simulator TOUGH2 (Pruess, 1991) is used for all fluid flow calculations. TOUGH2 is a fully implicit integrated finite difference code which solves the time dependent equations of mass and energy conservation in a porous medium, supplemented with appropriate constitutive relationships for the density, enthalpy and viscosity of liquid water and steam. The transport of fluid is described by Darcy's Law. The basic form of TOUGH2 contains a description of the thermophysical properties of water to 350°C and 80 MPa taken from the United Kingdom Steam Tables (1970), and can handle two-phase (liquid plus steam) flows by using vapour saturation as a primary variable in place of temperature. For applications involving higher temperatures and pressures (and the present work) , TOUGH2 has been extended by Kissling (1995) to include fluid properties at supercritical conditions to 2000°C and 300 MPa, using the NIST formulation (Haar, Gallagher and Kell, 1984).

Because of the large vertical dimension (30 km) of the model, it is necessary to add an extra term to the energy conservation equation to account for the change in gravitational energy of the fluid as it ascends to the surface (in the case of an upflow). This is done by adding an additional term gz to the fluid enthalpy, where g is the acceleration due to gravity (9.81 ms^{-2}), and z is the depth of the each TOUGH2 element with respect to the surface. The effect of this change is particularly striking in regions of downflow from the surface. The 'traditional' equations predict that in such regions the temperature will actually decrease to below freezing point, whereas the additional term ensures a modest increase in temperature with depth.

The TOUGH2 model domain is 150 km wide and 30 km deep. This is 'patched' onto the SULEC model domain directly above the heat flux anomaly. The TOUGH2 mesh consists of 4500 1 km × 1 km model elements. Surface topography is implemented by removing those elements whose centres lie above the ground surface, as defined in the SULEC model. These elements are given 'atmospheric' conditions of P = 1 bar and T = 15°C. The lateral boundaries of the model are set to admt no flow of fluid or heat. Temperatures and fluid pressures from SULEC are transferred directly onto this mesh, as are the rock types and the brittle-ductile state, as described in the next section.

There are five distinct rock types used in the model. These can be classified as 'Crustal', in either brittle or ductile state, and 'Mantle', also in brittle or ductile state, and the remaining rock type is 'Partial Melt'. Here, we run three different TOUGH simulations (labelled A, B and C in Table 4) with a range of permeabilities for the crustal rocks, to explore the effect of these on the evolution of the overlying hydrothermal system. The permeabilities of the mantle and partial melt rocks are fixed in these simulations. These permeabilities are shown in Table 4.

Table 4. Permeabilities used in TOUGH models.

Rock Type (model)	Permeability (m^2, $k_x = k_y$)
Brittle Crust (A)	10^{-15}
Ductile Crust (A)	10^{-16}
Brittle Crust (B)	10^{-16}
Ductile Crust (B)	10^{-17}
Brittle Crust (C)	$3x10^{-15}$
Ductile Crust (C)	10^{-16}
Brittle Mantle (A, B, C)	$5x10^{-17}$
Ductile Mantle (A, B, C)	$5x10^{-18}$
Partial Melt (A, B, C)	$1x10^{-18}$

3.3 One-way coupling of the two codes

We use SULEC to predict the change in crustal properties and the evolution in the brittle-ductile transition. For specified SULEC output times, the basal heat-flow, material properties, degree of melting, brittle and ductile material evolution and rift geometry and an inferred permeability distribution for the upper 30 km of the crust are passed to TOUGH2, and the evolution of fluid flow is followed for 100-200 kyr. This is sufficient time for the pressure (and therefore the flow field) to equilibrate, and to adjust to the imposed permeabilities. This one-way

coupling allows us to examine the changing fluid flow regime predicted by TOUGH2 for the crust as the rift evolves.

Some aspects of this coupling require further explanation. Firstly, the SULEC model predicts the presence of some partial melt within the crust, and some account of this must be taken in the TOUGH2 model. Our approach is to assume that this material has very low permeability to flow, and that it is a source of heat and fluid. The heat flux is calculated according to the change in partial melt from one timestep to the next, using a melt density of 2500 kgm^{-3} and a latent heat of 1 $MJkg^{-1}$. The fluid flux is then determined by assuming a constant rate of 0.1 kg/s/MJ, equal to the magmatic input to the TVZ (Giggenbach, 1995). Secondly, to provide lower boundary conditions for the TOUGH2 model domain, SULEC calculates the 'basal' fluxes of fluid and heat at the depth (30 km) corresponding to this boundary. These fluxes, the additional source terms which come from the treatment of partial melt, rock types, a brittle-ductile flag and the initial conditions are used to create a TOUGH2 model input file using a series of programs which overwrite parts of a dummy input file.

Finally, we emphasise that this is only a partial coupling, in that there is no feedback from the TOUGH2 fluid flow calculations into the thermo-mechanical model. Furthermore, at present we have only examined permeability changes in the crust associated with brittle-ductile behaviour.

4. RESULTS

4.1 SULEC

The setup of the thermo-mechanical model is shown in Figure 2(a). We chose a period of 2 My of tectonic quiescence to allow the basal heat-flow and mass flux anomaly (at 120 km depth) to propagate into the thermo-mechanical model. After this time, we imposed extensional boundary conditions to represent rifting.

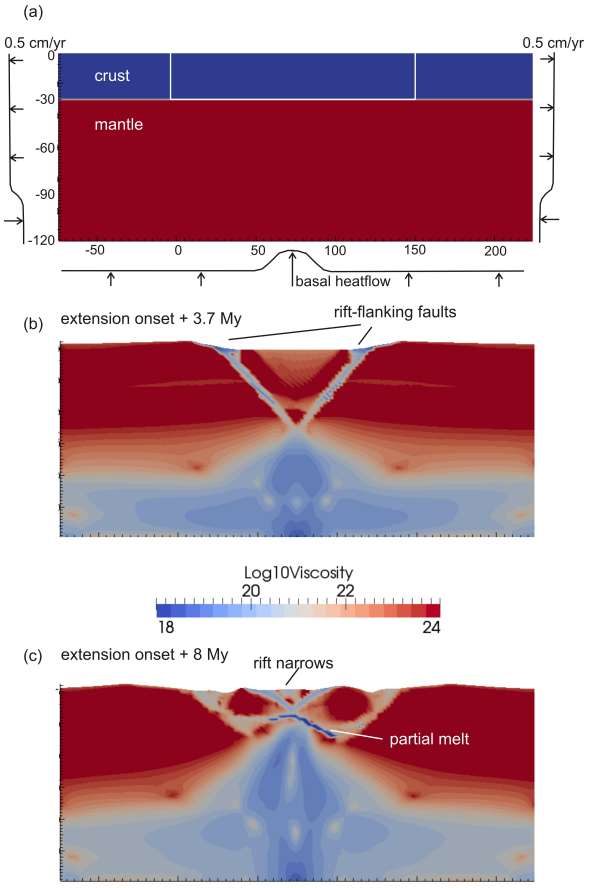


Figure 2. a) Setup of thermo-mechanical model with initial crustal thickness of 30 km (blue), and mantle (red). Elevated heat-flow is applied over a small region at the base. After a further 2 My, extensional boundary conditions are applied as shown. The white box outlines the area modelled with TOUGH2. (b) Log (effective viscosity) 3.7 My after extension starts showing developing of steep rift-flanking faults localised above heat-flow anomaly. (c) Log (effective viscosity) 8 My after extension starts. The locus of deformation has moved inward to the central faults, which have been rotated to shallow angles. A small zone of partial melt has developed at the base of the crust.

Figure 2(b) shows effective viscosity after 3.7 My of extension. Red colours indicate high strength crust and mantle whereas blue shows areas of low creep strength (mantle) and/or areas that have experienced brittle faulting. Note that the viscosity is self-determined in the model according to ambient fluid pressures, strain-rates, pressure and temperature at each time. The plot shows the classic 'Christmas tree' strength profile where pressure-sensitive brittle behaviour gives way to lower-strength creep with increasing temperature and pressure. The low-viscosity zones in the shallow lithosphere represent strain-softened rift-flanking faults, dipping at about 50 degrees and spaced ca. 80 km apart at the surface.

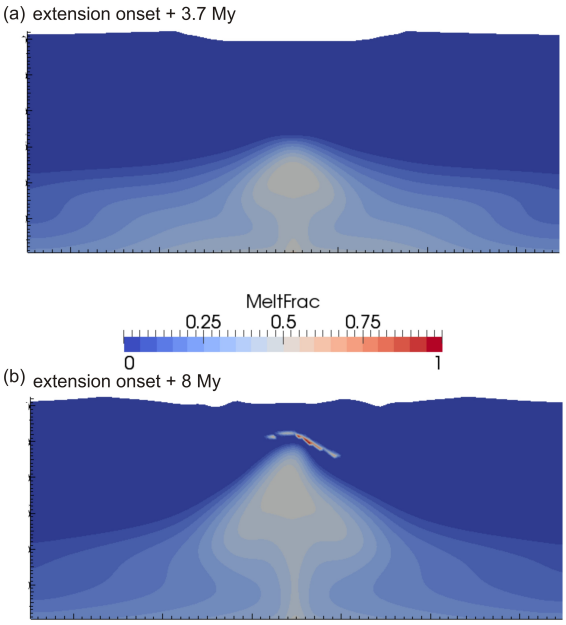


Figure 3. Partial melt evolution in the thermo-mechanical model.

The low viscosity zone at greater depths is partly controlled by development of partial melt in the mantle (Figure 3(a)). In turn, the location and development of a rift in the centre of the model is controlled by this partial melt and thus by the imposed basal heat flow anomaly at 120 km depth, which represents the flux of heat and fluids from subducted sediments.

With further extension (Figure 2(c), 8 My) the rift narrows as the lithosphere necks. A zone of partial melt has developed near the base of the crust, causing very low viscosities there which help to localise the deformation (Figure 3(b)).

The timescale of rifting in this model compared to the Taupo Rift is too long. Further experiments are needed to assess which factors control the timescale of melting and rifting, but we expect that the transfer of additional heat by fluids and advection of partial melt is an important process, missing in this model, which would considerably shorten the timescale of rift localisation.

Nevertheless, as a starting model, we can use "snapshots" of the thermo-mechanical model to feed into a more detailed shallow model of hydrothermal circulation using TOUGH2.

4.2 TOUGH2

Parameter values as described in section 3.3 are passed from SULEC to TOUGH2 after 8 My of rift evolution (Figure 2(c), Figure 3(b)). This provides the initial conditions for TOUGH2 models A, B and C (permeabilities as defined in Table 4). In all three cases, the brittle crust has a higher permeability than the ductile crust. These models are run for 200 kyr.

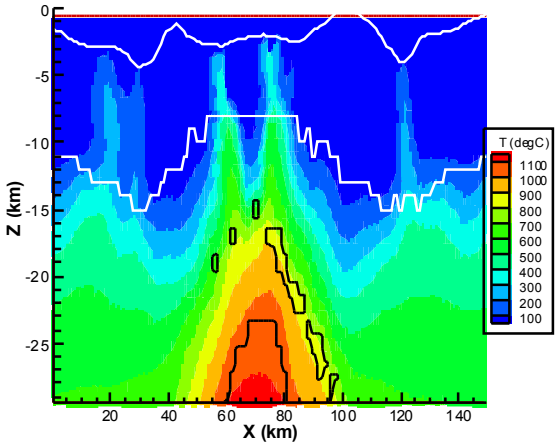


Figure 4. Temperature distribution calculated from TOUGH2 for model A, at 200 kyr. The upper and lower white lines show the locations of the model surface and the brittle-ductile transition, while the black contours show zones of partial melt. Note that the vertical exaggeration is 5x.

Figure 4 shows the resulting temperature distribution for model A after 200 kyr. The main features are: (1) elevated temperatures above and within the zone of partial melt (Figure 3(b)); (2) two hot narrow plumes rising to the surface on either side of the thermal anomaly and nucleating near the brittle-ductile transition; (3) a number of cold downflow zones between the plumes and on either side which reach the depth of the brittle-ductile transition and provide recharge for the plumes.

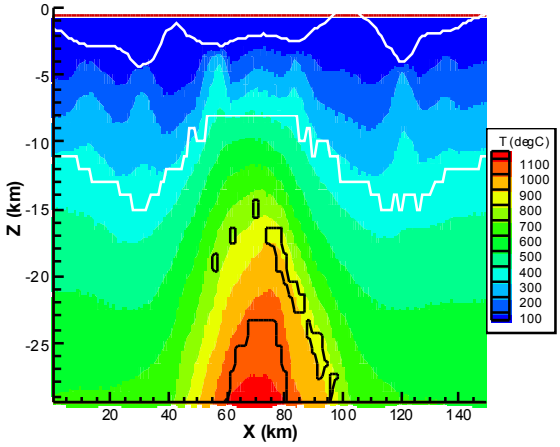


Figure 5. Temperature distribution calculated from TOUGH2 for model B, at 200 kyr. The upper and lower white lines show the locations of the model surface and the brittle-ductile transition, while the black contours show zones of partial melt. Note that the vertical exaggeration is 5x.

In Figure 5, we reduce the permeability of both brittle and ductile crust by a factor of 10 compared to model A, with all other permeabilities remaining the same. This suppresses the formation of the hydrothermal plumes; instead, a broad

upflow zone develops above the region of partial melt in crust and mantle.

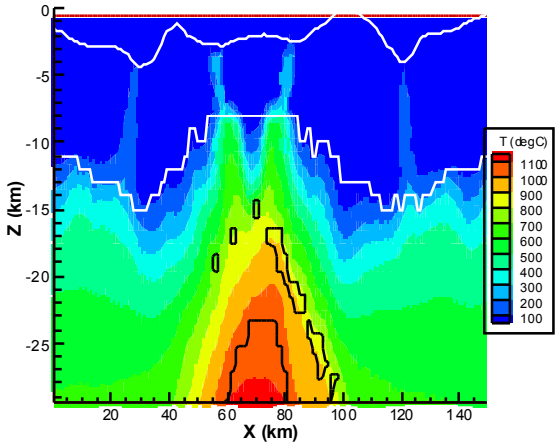


Figure 6. Temperature distribution calculated from TOUGH2 for model C, at 200 kyr. The upper and lower white lines show the locations of the model surface and the brittle-ductile transition, while the black contours show zones of partial melt. Note that the vertical exaggeration is 5x.

Finally, if instead we increase the ratio of brittle to ductile crustal permeability (model C), all of the plumes from model A are still present, but they are significantly cooler. This is presumably because the higher brittle permeability allows higher flows and recharge by cool surface water (Figure 6).

5. DISCUSSION AND CONCLUSIONS

At this stage the results demonstrate "proof of concept" for one-way coupling between tectonic and fluid codes: the evolving melt distribution (fluid and heat source), crustal architecture, and brittle-ductile transition from SULEC have been successfully used to drive hydrothermal circulation in TOUGH2. The basic 2D models demonstrate robust features that have been seen in earlier TOUGH2 models, for example the presence of narrow hydrothermal plumes with relatively high temperatures and the existence of large downflow regions which provide the recharge for these plumes (Kissling et al., 2009). The advantage of our scheme is that it allows us to gauge how fluid flow patterns may have evolved over millions of years during the evolution of a rift.

One improvement to earlier models is that the temperatures near the surface in the plumes in models A and C are hotter than in previous large scale models (e.g. Kissling and Weir, 2005). The temperatures in these plumes are ~250˚C at 2 km below the surface, which is in reasonable agreement with measured temperatures in some TVZ geothermal fields. This is perhaps in part caused by more realistic modelling of the heat source and its relation to the brittle-ductile transition, but we note that a) the model resolution (1 km) is still poor compared to the width of these plumes and b) we have investigated a limited set of simple models where permeabilities are only modified according to the brittle-ductile behaviour of the rocks.

Several additional improvements would further aid the one-way coupling:

- Permeability could also be made a function of stress and strain-rate. For example, if zones of high extensional deviatoric stress open up fluid pathways and enhance permeability, this could be important to fluid flow evolution;
- Better matching of fluid and thermal parameter descriptions between the two codes;
- Modelling of melt needs improvement, including a better way of defining conditions under which melt occurs and its effect on viscosity and other rheological parameters.

ACKNOWLEDGEMENTS

Funding for this work was provided from the GNS 'Hotter and Deeper' (WK) and GHZ and GNS Science Development Projects (SE). We thank Pilar Villamor, David Dempsey, Colin Wilson, Julie Rowland, Stephen Bannister, Andrew Rae, Wiebke Heise and Grant Caldwell for helpful discussions. The code SULEC was jointly written by Susan Ellis and Susanne Buiter from Norwegian Geological Survey.

REFERENCES

Bibby, H.M., Caldwell, T.G., Davey, F.J. and Webb, T.H.: Geophysical evidence on the structure of the Taupo Volcanic Zone and its hydrothermal circulation. *J. Volcan. Geotherm. Res.* 68, 29-58. (1995).

Bibby HM, G. F. Risk, T.G. Caldwell , Heise W. & S.L. Bennie.: Resistivity structure of western Taupo Volcanic Zone, New Zealand, *N.Z. J. Geol. Geophys*., 51, 231–244 (2008).

Browne, P.R.L.: Minimum age of the Kawerau geothermal field, North Island, New Zealand. *J. Volcan. Geotherm. Res.* 6, 213-215. (1979).

Bryan, C.J., Sherburn, S., Bibby, H.M., Bannister, S.C., Hurst, A.W.: Shallow seismicity of the central Taupo volcanic zone, New Zealand: its distribution and nature. NZJ66, 42, 533-542 (1999).

Eberhart-Phillips, D.; Reyners, M.E.; Chadwick, M.P.; Stuart, G.: Three-dimensional attenuation structure of the Hikurangi subduction zone in the central North Island, New Zealand. *Geophysical Journal International,* 174(1): 418-434; doi: 10.1111/j.1365-246X.2008.03816.x (2008).

Freed, A., and Bürgmann, R., 2004. Evidence of power-law flow in the Mojave desert mantle. *Nature*, 430, 548-551.

Gerya, T.V., Yuen, D.A.: Characteristics-based marker-in-cell method with conservative finite-differences schemes for modeling geological flows with strongly

variable transport properties. *Phys. Earth Planet. Inter*., 140, 293-318 (2003).

Giggenbach, W.F.: Variations in the chemical and isotopic compositions of the fluids discharged from the Taupo volcanic Zone, New Zealand. *J. Volcan. Geotherm. Res.* 68, 89-116 (1995); doi:10.1016/0377-0273(95)00009-J

Gleason, G.C., and Tullis, J.: A flow law for dislocation creep of quartz aggregates determined with molten salt cell. *Tectonophysics*, 2471-23. (1995).

Grindley, G.W.: The geology, structure and exploitation of the Wairakei geothermal field, Taupo, New Zealand. Geol. Survey *Bulletin*. 75, 131 pp (1965).

Haar, L., Gallagher, J.S., Kell, G.S.: NBS/NRC Steam Tables, 320 pp. Hemisphere Publishing, New York (1984).

Harrison, A., and White, R.S., 2006. Lithospheric structure of an active backarc basin: the Taupo Volcanic Zone, New Zealand. *Geophys J Int*, 167, 968-990, (2006).

Hayes, G., Reyners, M., Stuart, G.: The Waiouru, New Zealand, earthquake swarm: persistent mid-crustal activity near an active volcano. *Geophys. Res. Lett.* 31, L19613 (2004).

Heise, W., Caldwell, T.G., Bibby, H.M, and Bennie, S.L.: Three- dimensional electrical resistivity image of magma beneath an active continental rift, Taupo Volcanic Zone, New Zealand. *Geophys. Res. Lett.,* 37, doi:10.1029/2010GK043110 (2010).

Kaus B.J.P, Mühlhaus H., May D.A., 2010. A stabilization algorithm for geodynamic numerical simulations with a free surface. Phys. Earth Planet. Inter. 181, 12-20. (2010).

Kissling, W.M.: Extending MULKOM to super-critical temperatures and pressures. *Proc. World Geothermal Congress 1995*, Florence, Italy. 1687-1690. (1995).

Kissling, W.M. and Weir, G.J.: The Spatial Distribution of the Geothermal Fields in the Taupo Volcanic Zone, New Zealand. *J. Volcan. Geotherm. Res.* 145, 136-150. (2005).

Kissling, W., Ellis, S., Charpentier, F. and Bibby, H.: Convective Flows in a TVZ-like Setting with a Brittle/Ductile Transition. *Transport in Porous Media*, 77, 335-355. (2009).

Pelletier, D., Fortin, A., Camarero, R.: Are FEM solutions of incompressible flows really incompressible? (or how simple flows can cause headaches!). *Int. J. Num. Meth. Fluids* ,9, 99-112 (1989).

Pruess, K.: TOUGH2 – A General Purpose Numerical Simulator for Multi-phase fluid and heat flow. Report LBL-29400. Lawrence Berkeley Laboratory, 79pp. (1991).

Quinquis, M.E.T., Buiter, S.J.H., Ellis, S.: The role of boundary conditions in numerical models of subduction zone dynamics, *Tectonophys.* 497, 57-70, doi:10.1016/j.tecto.2010.11.001 (2011).

Rowland, J.V., and Sibson, R.H.: Extensional fault kinematics within the Taupo Volcanic Zone, New Zealand: soft-linked segmentation of a continental rift system. *New Zealand Journal of Geology & Geophysics,* 44, 271-283, (2001).

Rowland, J.V., Wilson, C.J.N. & Gravley, D.M. Spatial and temporal variations in the mechanics of magma-assisted rifting, Taupo Volcanic Zone, New Zealand. *Journal of Volcanology and Geothermal Research* 190, 89-108, doi:10.1016/j.jvolgeores.2009.05.004. (2010).

Rowland, J.V. and Sibson, R.H.: Structural controls on hydrothermal flow in a segmented rift system, Taupo Volcanic Zone, New Zealand. *Geofluids* 4, 259-283. (2004) .

Sherburn, S. and White, R.S.: Crustal seismicity in Taranaki, New Zealand, using accurate hypocenters from a dense network. *Geophys. J. Int.* 162, 494-506. (2005) .

Villamor, P., Berryman, K., Ellis, S., Nairn, I., Langridge, R., and Schreurs, G.: *in prep*. Rapid onset of narrowing and propagation of an intra-arc rift: the Taupo Rift, New Zealand.

Villamor, P., and Berryman, K.: A late Quaternary extension rate in the Taupo Volcanic Zone, New Zealand, derived from fault slip data. *NZ J. Geol. Geophys.* 44, 243-269. (2001).

Wallace, L.M., Beavan, J., McCaffery, R., Darby, D.: Subduction Zone coupling and tectonic block rotations in the North Island, New Zealand. *J. Geophys. Res.* 109, B12406 (2004).

Wilson, C.J.N., Houghton, B.F., McWilliams, M.O., Lanphere, M.A., Weaver, S.D., Briggs, R.M.: Volcanic and structural evolution of Taupo Volcanic Zone, New Zealand: a review. *J. Volcan. Geotherm. Res*. 68, 1-28. (1995).